Ocean Sci. Discuss., 10, 1971–1996, 2013
www.ocean-sci-discuss.net/10/1971/2013/
doi:10.5194/osd-10-1971-2013


Ocean Science
Discussions
Open Access



# First air–sea gas exchange laboratory study at hurricane wind speeds

**K. E. Krall[1] and B. Jähne[1,2]**

[1]Institute of Environmental Physics, University of Heidelberg, Im Neuenheimer Feld 229, 69120 Heidelberg, Germany
[2]Heidelberg Collaboratory for Image Processing, University of Heidelberg, Speyerer Straße 6, 69115 Heidelberg, Germany

Received: 2 October 2013 – Accepted: 18 October 2013 – Published: 5 November 2013

Correspondence to: K. E. Krall (kerstin.krall@iup.uni-heidelberg.de)

Published by Copernicus Publications on behalf of the European Geosciences Union.

## Abstract

In a pilot study conducted in October and November 2011, air–sea gas transfer velocities of the two sparingly soluble trace gases hexafluorobenzene and 1,4-difluorobenzene were measured in the unique High-Speed Wind-Wave Tank at Kyoto University, Japan. This air–sea interaction facility is capable of producing hurricane strength wind speeds of up to $u_{10} = 67\,\mathrm{m\,s^{-1}}$. This constitutes the first lab study of gas transfer at such high wind speeds. The measured transfer velocities $k_{600}$ spanned two orders of magnitude, lying between $11\,\mathrm{cm\,h^{-1}}$ and $1180\,\mathrm{cm\,h^{-1}}$ with the latter being the highest ever measured wind induced gas transfer velocity. The measured gas transfer velocities are in agreement with the only available dataset at hurricane wind speeds (McNeil and D'Asaro, 2007). The disproportionately large increase of the transfer velocities found at highest wind speeds indicates a new regime of air–sea gas transfer, which is characterized by strong wave breaking, enhanced turbulence and bubble cloud entrainment. It was found that tracers spanning a wide range of solubilities and diffusivities are needed to separate the effects of enhanced surface area and turbulence due to breaking waves from the effects of bubble and spray mediated gas transfer.

## 1 Introduction

Ocean regions, where strong winds usually occur, play an important role in global $CO_2$ budgets, see Bates et al. (1998). Therefore, a better understanding of gas transfer at high wind speed conditions is essential. Field measurements of air–sea gas exchange velocities under hurricane wind speed conditions are sparse due to difficulties of sampling under extreme wind conditions. During hurricane Frances in 2004, McNeil and D'Asaro (2007) measured three transfer velocities of $O_2$ using unmanned floats at wind speeds larger than $25\,\mathrm{m\,s^{-1}}$, with the highest wind speed being $50.4\,\mathrm{m\,s^{-1}}$.

High wind speeds are associated with the presence of breaking waves. These enhance turbulence near the water surface and generate spray and bubble plumes, which





OSD
10, 1971–1996, 2013

increases gas fluxes, see for instance Monahan and Spillane (1984) and Farmer et al. (1993). Breaking waves enhance gas transfer by several mechanisms. The water surface, across which gas is transferred, is enlarged by waves, and by breaking, waves enhance near surface turbulence. Bubbles and spray provide a limited, mostly short-lived volume of air or water associated with an additional surface area, over which gas transfer can occur (Memery and Merlivat, 1985). And by floating through air and water and bursting through the water surface, bubbles and spray enhance turbulent mixing near the water surface.

Wind-wave tanks provide an alternative to measurements in the field. All the inconveniences and dangers associated with measurements in the field during hurricane wind speed conditions are virtually non-existent in a lab setup.

## 2 Air–sea gas transfer

The gas transfer velocity $k$, along with the net gas flux $j$, is commonly used to describe the gas transfer process across the air–sea boundary

$$j = k\Delta c = k(c_{\mathrm{w}} - \alpha c_{\mathrm{a}}) \tag{1}$$

with the tracer's air and water side concentrations, $c_{\mathrm{a}}$ and $c_{\mathrm{w}}$, respectively, and the tracer's dimensionless solubility $\alpha$.

For a sparingly soluble tracer, a dependency of the transfer velocity $k$ on the water sided friction velocity $u_*$, a measure for momentum input into the water, is commonly assumed in the form

$$k \propto u_* Sc^{-n} \tag{2}$$

with the tracer's dimensionless Schmidt number $Sc = \nu/D$, the ratio between the kinematic viscosity of water $\nu$ and the tracer's diffusivity in water $D$. The Schmidt number exponent $n$ is 2/3 in the case of a smooth water surface and 1/2 for a rough and wavy





OSD
10, 1971–1996, 2013

surface. More thorough derivations of Eq. (2) can be found in Deacon (1977); Coantic (1986) and Jähne et al. (1989).

Equation (2) can be used to compare the transfer velocities of two tracers A and B under the same conditions in the form of Schmidt number scaling,

$$\frac{k_A}{k_B} = \left(\frac{Sc_A}{Sc_B}\right)^{-n}. \tag{3}$$

On the ocean, the gas transfer velocity depends on many different factors such as wind speed, fetch, the presence of surface active material and atmospheric stability. Wind speed has been identified as the main forcing factor. Many different empirical wind speed–gas transfer velocity parameterizations have been proposed in the last decades, for instance Liss and Merlivat (1986); Wanninkhof (1992); Nightingale et al. (2000); McGillis et al. (2001); Wanninkhof et al. (2009). These were all developed in the wind speed region below $15\,\mathrm{m\,s^{-1}}$, where most of them agree reasonably well with each other. Extending these parameterizations to wind speeds observed in a hurricane, see Fig. 1, paints a different picture with large deviations between the different parameterizations. At a wind speed of $50\,\mathrm{m\,s^{-1}}$, the deviations between the highest and the lowest predicted transfer velocity is more than one order of magnitude. This highlights the very limited applicability of gas transfer – wind speed parameterizations in hurricane conditions. The only parameterization available for hurricane wind speeds by McNeil and D'Asaro (2007), who measured gas transfer velocities during hurricane Frances, is also shown in Fig. 1.

At high wind speeds, breaking waves generate spray and bubbles. Gas transfer due to single bubbles is well studied experimentally, see for instance Mori et al. (2002) and Vasconcelos et al. (2002), as well as in models, see Memery and Merlivat (1985). The impact of spray on the gas exchange velocity, however, is not studied well. In most models of gas exchange at high wind speeds, the effects of breaking waves, spray and bubble clouds are combined into the breaking waves mediated transfer velocity, $k_b$. Then it is assumed, that the total gas transfer velocity $k$ can be split up into direct





OSD
10, 1971–1996, 2013

transfer through the surface $k_s$ and the breaking mediated transfer velocity $k_b$,

$$k = k_s + k_b, \tag{4}$$

see Merlivat and Memery (1983). The breaking waves part of the transfer velocity $k_b$ is usually parameterized using the whitecap coverage parameter, which describes the percentage of the total water surface area covered in whitecaps. Examples of parameterizations of $k_b$ can be found in Keeling (1993) and Asher et al. (1996). More complex, but still partially empirical models are also available, see for instance Woolf et al. (2007). All of the models of gas transfer at high wind speeds have in common, that the gas exchange of a specific tracer does not only depend on the Schmidt number but also on the solubility. Assuming tracers with the same Schmidt number, the transfer velocity due to breaking waves in these empirical models is higher for the tracer with the lower solubility.

## 3 Method

Classical evasion experiments, see for instance Jähne et al. (1979), were conducted in this study. In an evasion experiment, the decrease in concentration of a tracer, mixed into the water before the start of the experiment, is monitored over time. The simple approach described in Jähne et al. (1979) must be slightly modified and adapted to the Kyoto High-Speed Wind-Wave Tank to accommodate for water lost from the system due to spray.

Under the condition of a negligible air side concentration $\alpha c_a \approx 0$, and small solubility $\alpha$, as well as the choice of a tracer that is not in the water used to replace the water lost due to spray, the mass balance for a tracer in the water side is found to be

$$V_w \dot{c}_w = -(Ak + \dot{V}_w) c_w. \tag{5}$$

In this equation, the mass of the tracer in water is expressed using the water side concentration $c_w$. $A$ denotes the water surface area, $V_w$ the total water volume and $\dot{V}_w$





OSD
10, 1971–1996, 2013

is the rate of water inflow to replace water lost from the flume due to spray being blown out of the tank. The Kyoto High-Speed Wind-Wave Tank is an open facility, meaning fresh ambient air is blown over the water surface once and then removed from the system. Choosing a tracer that is not present in ambient air, the condition of a negligible air side concentration $\alpha c_a \approx 0$, can be met.

Equation (5) can be easily solved,

$$c_w(t) = c_w(0) \cdot \exp\left(-\left(k \cdot \frac{A}{V_w} + \frac{\dot{V}_w}{V_w}\right) \cdot t\right), \tag{6}$$

with $c_w(0)$ being the water side concentration at time $t = 0$.

The time constant $\tau$ of this equation is defined as

$$\frac{1}{\tau} := k \cdot \frac{A}{V_w} + \frac{\dot{V}_w}{V_w}. \tag{7}$$

This time constant $\tau$ is acquired from an exponential fit of Eq. (6) to the time series of measured concentrations. The water volume $V_w$, the water surface area $A$, as well as the leak rate $\lambda = \dot{V}_w / V_w$ are known or measured during an experiment. The transfer velocity can then be calculated as

$$k = \left(\frac{1}{\tau} - \lambda\right) \cdot \frac{V_w}{A}. \tag{8}$$

## 4 Experiments

### 4.1 Tracers

The tracers were chosen such that their diffusivity in water, and thus their Schmidt numbers, were similar, while their solubility differed. Because UV absorption spectroscopy





OSD
10, 1971–1996, 2013

was used to measure tracer concentrations, tracers which exhibit a high extinction coefficient in the UV range as well as distinctly different spectra were chosen. To keep the mass balance described in Sect. 3 simple, the tracers were required to not be present in ambient air, as well as not present in the tap water. The tracers chosen by these criteria were hexafluorobenzene (HFB) and 1,4-difluorobenzene (DFB). Table 1 lists properties of the tracers as well as carbon dioxide as a reference.

## 4.2 Experimental setup

### 4.2.1 The Kyoto High-Speed Wind-Wave Tank

The Kyoto High-Speed Wind-Wave Tank has a linear flume shape, see Fig. 2. The water flume is 80 cm wide, has a total length of 15.7 m with 12.9 m being exposed to the wind. The total height is 1.6 m, with up to 0.8 m being filled with tap water. The wind is generated by a radial fan. The maximum wind speed that can be reached is $u_{10} = 67.1\,\mathrm{m\,s^{-1}}$. Before the wind enters the air side of the tank, it is passing through a honeycomb structure to minimize large eddies. The air is taken from the room surrounding the wind-wave tank and guided out of the building after it was blown over the water.

There is an external water tank available that holds up to $7\,\mathrm{m}^3$ of water, which is connected to the wind-wave flume by two pipes. A pump draws the water out at the downwind end of the flume and into the water tank, and another pump draws the water out of the tank and into the upwind end of the wind-wave flume. For all lower wind speed settings, the amount of water coming out of the lab's water supply lines is sufficient to replace the water lost due to spray. At the highest wind speed setting, the external tank was used as a buffer to keep the water level constant inside the wind-wave tank. Trace gases can be mixed into the water by operating both pumps and thus cycling the water between the external tank and the wind-wave flume.





OSD
10, 1971–1996, 2013

### 4.2.2 Concentration measurement

Tracer concentrations in the water were monitored using UV absorption spectroscopy. Water was sampled at a fetch of about 6.5 m at a water height of approximately 35 cm with a rate of 7 to 10 L min$^{-1}$. The approximate sampling location is marked in Fig. 2. Because air bubbles, generated by breaking waves would have scattered the light out of the UV spectroscopic measuring cell, it was chosen to not spectroscopically analyze the water directly, but to equilibrate the water with a small parcel of air first, and analyze this air. The water extraction and equilibration setup is shown in Fig. 3. A membrane equilibrator called an oxygenator (*Jostra Quadrox* manufactured by *Maquet*, Hirrlingen, Germany) was used to equilibrate the water with the air. In Krall (2013), the performance and applicability of the oxygenator setup is validated from geometrical consideration as well as test experiments. Air is cycled around the closed air loop at a rate of about 150 mL min$^{-1}$. During the measurements, the valves were set such, that no outside air could enter or leave the air loop. During preparation of the experiment, the valves allowed sampling of ambient air to estimate the background. In addition, the water temperature was monitored.

The gas sampling cell is made of a 1 m long quartz glass tube with an inner diameter of 3 mm. Light produced by a deuterium lamp enters the tube through a quartz glass lens with focal length of 5 cm and a quartz glass window. It leaves the measuring cell through another quartz glass window and lens to be focused on a glass fiber. This glass fiber is connected to a UV spectrometer (*Maya2000 Pro* by *Ocean Optics*, Dunedin, USA). This spectrometer can resolve wavelengths from 190.5 nm to 294.1 nm with a resolution of approximately 0.05 nm. About one spectrum was acquired per second.

During data evaluation, one absorbance value per tracer is calculated from each spectrum in a process described in detail in Krall (2013). Beer's law states that the absorbance $A$ of a tracer is directly proportional to the concentration in the measured air parcel, $c_a$. According to Henry's law, the air side concentration is proportional to the





OSD
10, 1971–1996, 2013

water side concentration $c_w$, thus $A \propto c_a \propto c_w$. Because only the change in concentration over time is relevant to measure the gas transfer velocity, see Eqs. (6) and (8), no absolute calibration that converts absorbance into the water side concentrations is needed. Equation (6) can then be converted into the form

$$\frac{c_w(t)}{c_w(0)} = \frac{A(t)}{A(0)} = \exp\left(-\frac{t}{\tau}\right), \tag{9}$$

with the time constant $\tau$ that is needed to calculate the gas transfer velocities, see Eq. (8).

### 4.3 Experimental conditions

A total of 21 experiments at 9 different fixed wind speeds were performed. The wind generator's rotational frequency $f_{fan}$ was set and kept constant for each condition. The free stream wind speed $u_{inf}$, the air sided friction velocity $u_*$ as well as the wind speed at a height of 10 m $u_{10}$ that is commonly used as a reference were not measured during the presented campaign, but taken from a table kindly provided by the Japanese colleagues. Water height $h_w$ was measured at the wind inlet before and after each experiment with no wind and no waves. Typically, both water height values differed by no more than 1 %. This ensured that the rate of inflowing water $\dot{V}_w$ was equal to the amount of water lost due to spray as required by the method, see Sect. 3. The conditions used are listed in Table 2. Transfer velocities of both tracers were measured in parallel in each of the experiments, with the exception of one experiment at $f_{fan}$=600, where only the absorbance time series of DFB could be evaluated.





OSD
10, 1971–1996, 2013

## 5 Results

### 5.1 Comparison with the gas exchange model and previous measurements

A total of 41 transfer velocities were measured, 21 of which for DFB and 20 for HFB. Figure 4 shows the measured transfer velocities for both tracers vs. the transfer velocities predicted by Eq. (2). The momentum transfer resistance parameter $\beta$ was assumed to be 6.7, see Krall (2013). The Schmidt number exponent was chosen to be $n = 0.5$ at medium to high wind speeds. However, for the two lowest wind speeds of $7\,\mathrm{m\,s^{-1}}$ and $12.1\,\mathrm{m\,s^{-1}}$ the exponent was set to a value of 0.55, to compensate for the smooth water surface visually observed at low fetches during this wind speed conditions. For the low friction velocities of up to $u_* < 6\,\mathrm{cm\,s^{-1}}$, which corresponds to a wind speed of $u_{10} < 35\,\mathrm{m\,s^{-1}}$ and transfer velocities around $80\,\mathrm{cm\,s^{-1}}$, the measured transfer velocities agree well with the transfer model's prediction. At higher wind speeds, the measured transfer velocities exceed the ones expected from Eq. (2) by up to around 340 % (HFB) and 220 % (DFB).

Figure 5 shows the transfer velocities, scaled to a Schmidt number of 600 using Schmidt number scaling (Eq. 3) in comparison with the data by McNeil and D'Asaro (2007) acquired on the open ocean, including their proposed parameterization. Within the margin of errors, both data sets agree surprisingly well.

### 5.2 Enhancement at highest wind speeds

Vlahos et al. (2011) present measured transfer velocities of dimethylsulfide (DMS), which show a decrease in the gas transfer velocity when bubble clouds are present at high wind speeds. For both tracers used in this study, this decrease is not observed. Up to a wind speed of $35\,\mathrm{m\,s^{-1}}$, the gas transfer velocity is roughly proportional to $u_{10}^{1.1}$. For higher wind speeds, the proportionality changes to $k \propto u_{10}^{3}$ for DFB and $k \propto u_{10}^{3.6}$ for HFB, see Fig. 6. This clearly indicates the start of a new regime of air sea gas exchange starting at around $35\,\mathrm{m\,s^{-1}}$.





OSD
10, 1971–1996, 2013

At highest wind speeds, the transfer velocity of HFB increases stronger than the one of DFB, as indicated by the different slopes in Fig. 6. To quantify this, an enhancement factor $E_f$ can be defined by

$$E_f := \frac{k_{600,\mathrm{HFB}} - k_{600,\mathrm{DFB}}}{k_{600,\mathrm{DFB}}} \times 100\,\%. \tag{10}$$

Figure 7 shows the enhancement factor $E_f$, averaged on a condition basis. Up to a wind speed of around 40 m s$^{-1}$, no enhancement is observed. Above 40 m s$^{-1}$, however, the transfer velocity of HFB is up to 40 % larger than that of DFB with a clear wind speed dependence. This enhancement is expected from bubble models, see Sect. 2, with the less soluble tracer HFB ($\alpha$ = 1.0 at 20 °C) having larger transfer velocities than the slightly higher soluble tracer DFB ($\alpha$ = 3.08 at 20 °C).

## 6 Conclusions

The transfer velocities at hurricane strength wind speeds were found to be extremely high. The measured transfer velocities were found to be in agreement with the only other data set of gas transfer at extreme wind speeds (McNeil and D'Asaro, 2007). In wind speeds higher than around 35–40 m s$^{-1}$, where frequent large scale wave breaking with bubble entrainment and spray generation occurs, the correlation between gas transfer velocities and wind speed was found to become steeper, indicating a new regime of air–sea gas exchange. The steepness of the relationship between the gas transfer velocity and the wind speed could be linked to the solubility of the tracer. The lower the solubility, the higher the transfer velocities measured.

The tracers used in this pilot study spanned only a small fraction of the Schmidt number – solubility parameter space, see Fig. 8. Because the covered parameter space is so small, general statements, applicable to all of the solubility and Schmidt number range would be highly speculative and is therefore omitted in this paper.





OSD
10, 1971–1996, 2013

The results of this pilot study confirm, that it is possible, to measure realistic air–sea gas exchange velocities in a wind-wave tank at hurricane wind speeds with the method described in this paper. However, due to the mentioned limitations in solubility and Schmidt number, a physical interpretation as well as physics based modeling will have to be suspended until further measurements with more tracers and detailed measurements of bubble and spray densities and of turbulence have been conducted. Choosing tracers covering the whole range of possible solubilities and Schmidt numbers is expected to expand the understanding of the processes involved in air–sea gas exchange at highest wind speeds. Partitioning the transfer velocity into a part due to enhanced turbulence at the water surface, and spray and bubble mediated gas transfer seems feasible in future studies at the Kyoto High-Speed Wind-Wave Tank.

## Appendix A

### Measured transfer velocities

Table A1 shows all measured transfer velocities, as well as mean water temperatures and Schmidt numbers of both tracers.

*Acknowledgements.* We thank all members of the Environmental Fluids and Thermal Engineering Lab at Kyoto University under the lead of S. Komori for providing exceptional working conditions and assistance during preparation and measurements, as well as N. Takagaki and K. Iwano for making wind speed, friction velocity and free stream velocity data available. We are grateful for the assistance of W. Mischler during all stages of the measurements. The financial support for this project by Mobility Networks within the Institutional Strategy ZUK49 “Heidelberg: Realising the Potential of a Comprehensive University” and by German Federal Ministry of Education and Research (BMBF) joint project “Surface Ocean Processes in the Anthropocene” (SOPRAN, FKZ 03F0611F) is gratefully acknowledged.

## References


Ambrose, D., Ewing, M. B., Ghiassee, N. B., and Sanchez Ochoa, J. C.: The ebulliometric method of vapour pressure measurement: vapour pressures of benzene, hexafluorobenzene, and naphthalene, J. Chem. Thermodyn., 22, 589–605, 1990. 1986

Asher, W. E., Karle, L. M., Higgins, B. J., Farley, P. J., Monahan, E. C., and Leifer, I. S.: The influence of bubble plumes on air–seawater gas transfer velocities, J. Geophys. Res., 101, 12027–12041, 1996. 1975

Bates, N. R., Knap, A. H., and Michaels, A. F.: Contribution of hurricanes to local and global estimates of air–sea exchange of $CO_2$, Nature, 395, 58–61, 1998. 1972

Coantic, M.: A model of gas transfer across air–water interfaces with capillary waves, J. Geophys. Res., 91, 3925–3943, 1986. 1974

Deacon, E. L.: Gas transfer to and across an air–water interface, Tellus, 29, 363–374, 1977. 1974

Farmer, D. M., McNeil, C. L., and Johnson, B. D.: Evidence for the importance of bubbles in increasing air–sea gas flux, Nature, 361, 620–623, 1993. 1973

Freire, M. G., Razzouk, A., Mokbel, I., Jose, J., Marrucho, I. M., and Coutinho, J. A. P.: Solubility of hexafluorobenzene in aqueous salt solutions from (280 to 340) *k*, J. Chem. Eng. Data, 50, 237–242, 2005. 1986

Jähne, B., Münnich, K. O., and Siegenthaler, U.: Measurements of gas-exchange and momentum-transfer in a circular wind–water tunnel, Tellus, 31, 321–329, 1979. 1975

Jähne, B., Heinz, G., and Dietrich, W.: Measurement of the diffusion coefficients of sparingly soluble gases in water, J. Geophys. Res., 92, 10767–10776, 1987. 1986

Jähne, B., Libner, P., Fischer, R., Billen, T., and Plate, E. J.: Investigating the transfer process across the free aqueous boundary layer by the controlled flux method, Tellus B, 41, 177–195, 1989. 1974

Keeling, R. F.: On the role of large bubbles in air–sea gas exchange and supersaturation in the ocean, J. Mar. Res., 51, 237–271, 1993. 1975

Kestin, J., Sokolov, M., and Wakeham, W. A.: Viscosity of liquid water in the range −8 °C to 150 °C, J. Phys. Chem. Ref. Data, 7, 941–948, 1978. 1986

Krall, K. E.: Laboratory Investigations of Air–Sea Gas Transfer under a Wide Range of Water Surface Conditions, Ph.D. Thesis, Institut für Umweltphysik, Fakultät für Physik und Astronomie, University of Heidelberg, 2013. 1978, 1980






OSD
10, 1971–1996, 2013

Liss, P. S. and Merlivat, L.: Air–sea gas exchange rates: introduction and synthesis, in: The role of air–sea exchange in geochemical cycling, edited by: Buat-Menard, P.. Reidel, Boston, MA, 113–129, 1986. 1974, 1989

McGillis, W. R., Edson, J. B., Hare, J. E., and Fairall, C. W.: Direct covariance air–sea $CO_2$ fluxes, J. Geophys. Res., 106, 16729–16745, 2001. 1974, 1989

McNeil, C. and D'Asaro, E.: Parameterization of air sea gas fluxes at extreme wind speeds, J. Marine Syst., 66, 110–121, 2007. 1972, 1974, 1980, 1981, 1989, 1993

Memery, L. and Merlivat, L.: Modelling of gas flux through bubbles at the air–water interface, Tellus B, 37, 272–285, 1985. 1973, 1974

Merlivat, L. and Memery, L.: Gas exchange across an air–water interface: experimental results and modeling of bubble contribution to transfer, J. Geophys. Res., 88, 707–724, 1983. 1975

Monahan, E. C. and Spillane, M. C.: The role of whitecaps in air–sea gas exchange Gas transfer at water surfaces, in: Gas Transfer at Water Surfaces, edited by: Brutsaert, W. and Jirka, G. H., 495–503, 1984. 1973

Mori, N., Imamura, M., and Yamamoto, R.: An experimental study of bubble mediated gas exchange for a single bubble, in: Gas Transfer at Water Surfaces, Geophysical Monograph, vol. 127, edited by: Donelan, M. A., Drennan, W. M., Saltzman, E. S., and Wanninkhof, R., 311–313, 2002. 1974

Nightingale, P. D., Malin, G., Law, C. S., Watson, A. J., Liss, P. S., Liddicoat, M. I., Boutin, J., and Upstill-Goddard, R. C.: In situ evaluation of air–sea gas exchange parameterization using novel conservation and volatile tracers, Global Biogeochem. Cy., 14, 373–387, 2000. 1974, 1989

Vasconcelos, J. M. T., Orvalho, S. P., and Alves, S. S.: Gas-liquid mass transfer to single bubbles: Effect of surface contamination, AIChE J., 48, 1145–1154, 2002. 1974

Vlahos, P., Monahan, E. C., Huebert, B. J., and Edson, J. B.: Wind-dependence of DMS transfer velocity: comparison of model with recent southern ocean observations, in: Gas Transfer at Water Surfaces 2010, edited by: Komori, S., McGillis, W., and Kurose, R., 313–321, 2011. 1980

Wanninkhof, R.: Relationship between wind speed and gas exchange over the ocean, J. Geophys. Res., 97, 7373–7382, doi:10.1029/92JC00188, 1992. 1974, 1989

Wanninkhof, R., Asher, W. E., Ho, D. T., Sweeney, C., and McGillis. W. R.: Advances in quantifying air–sea gas exchange and environmental forcing, Annu. Rev. Mar. Sci., 1, 213–244, 2009. 1974, 1989





OSD
10, 1971–1996, 2013

Woolf, D., Leifer, I., Nightingale, P., Rhee, T., Bowyer, P., Caulliez, G., de Leeuw, G., Larsen, S., Liddicoat, M., Baker, J., and Andreae, M.: Modelling of bubble-mediated gas transfer: Fundamental principles and a laboratory test, J. Marine Syst., 66, 71–91, 2007. 1975

Yaws, C. L.: Handbook of Transport Property Data, Gulf Publishing Company, 1995. 1986

Yaws, C. L. and Yang, H.-C.: Henry's law constant for compound in water, in: Thermodynamic and Physical Property Data, edited by: Yaws, C. L., Gulf Publishing Company, 181–206, 1992. 1986

Young, C. L. (Ed.): IUPAC Solubility Data Series, Oxides of Nitrogen, vol. 8, Pergamon Press, Oxford, England, 1981. 1986





OSD

10, 1971–1996, 2013

**Table 1.** Molar mass, solubility, diffusivity in water and Schmidt numbers of the tracers hexafluorobenzene (HFB) and 1,4-difluorobenzene (DFB) for a temperature of 20 °C. Also shown is $CO_2$ for comparison. [1]: calculated from mole fraction solubility from Freire et al. (2005) and vapor pressure from Ambrose et al. (1990). [2]: Yaws and Yang (1992). [3]: Young (1981). [4]: Yaws (1995) [5]: calculated from diffusion coefficients taken from Yaws (1995) and water viscosity taken from Kestin et al. (1987). [6]: Jähne et al. (1987).

| Name | $M$ g mol$^{-1}$ | $\alpha$ at 20 °C | $D$ $10^{-5}$ cm$^2$ s$^{-1}$ | $Sc$ |
|---|---|---|---|---|
| HFB | 186.1 | 1.0 [1] | 0.736[4] | 1360[5] |
| DFB | 114.1 | 3.08[2] | 0.815[4] | 1225[5] |
| $CO_2$ | 44.01 | 0.83[3] | 1.68[6] | 601[6] |





OSD
10, 1971–1996, 2013

**Table 2.** Experimental conditions used at the Kyoto High-Speed Wind-Wave Tank. $f_{fan}$ is the frequency of the wind generating fan, $u_*$ is the friction velocity, $u_{inf}$ denotes the free stream velocity, and $u_{10}$ is the wind speed at 10 m height. $\dot{V}_w$ is the leak rate. The number of repetitions of each of the conditions is labeled with $N$. One free stream velocity $u_{inf}$ was not measured (n.m.).

| $f_{fan}$ rpm | $u_*$ cm s$^{-1}$ | $u_{inf}$ m s$^{-1}$ | $u_{10}$ m s$^{-1}$ | $\dot{V}_w$ L min$^{-1}$ | $N$ | notes |
|---|---|---|---|---|---|---|
| 100 | 0.836 | 4.72 | 7.0 | 0 | 3 | |
| 150 | 1.50 | 10.36 | 12.1 | 0 | 1 | |
| 200 | 2.34 | 10.29 | 16.7 | 0 | 2 | |
| 250 | 3.10 | n.m. | 23.75 | 0 | 1 | |
| 300 | 5.19 | 16.26 | 29.8 | 0 | 3 | |
| 400 | 7.24 | 22.17 | 40.7 | 0 | 3 | |
| 500 | 8.23 | 28.47 | 48.0 | 3.5 | 2 | |
| 600 | 9.37 | 34.75 | 56.4 | 14.5 | 4 | only 3 experiments evaluable for HFB |
| 800 | 11.5 | 43.29 | 67.1 | 192 | 2 | $V_w$ decreased, external tank used |





OSD
10, 1971–1996, 2013

**Table A1.** Transfer velocities $k$ (not scaled to $Sc = 600$) measured in the Kyoto High-Speed Wind-Wave Tank for tracers 1,4-difluorobenzene (DFB) and hexafluorobenzene HFB and their respective uncertainties $\Delta k$. "n.m." means not measured. The wind speed $u_{10}$ and water sided friction velocity $u_*$, kindly provided by the Japanese colleagues, is also given. $T$ denotes the mean water temperature during the measurement. Schmidt numbers $Sc$ of the tracers at this temperature are also shown.

| Date | $u_{*,w}$ cm s$^{-1}$ | $u_{10}$ m s$^{-1}$ | $k_{HFB}$ cm h$^{-1}$ | $\Delta k_{HFB}$ cm h$^{-1}$ | $k_{DFB}$ cm h$^{-1}$ | $\Delta k_{DFB}$ cm h$^{-1}$ | $T$ °C | $Sc_{HFB}$ | $Sc_{DFB}$ | $n$ |
|---|---|---|---|---|---|---|---|---|---|---|
| 27 Oct 2011 | 9.38 | 56.4 | 369.5 | 14.8 | 332.1 | 12.8 | 17.5 | 1555 | 1403 | 0.5 |
| 28 Oct 2011 | 7.25 | 40.7 | 120.4 | 7.2 | 113.5 | 3.6 | 17.1 | 1590 | 1434 | 0.5 |
| 28 Oct 2011 | 9.38 | 56.4 | 415.3 | 23.3 | 299.2 | 14.0 | 17.1 | 1590 | 1434 | 0.5 |
| 31 Oct 2011 | 2.34 | 16.7 | 29.35 | 1.67 | 31.40 | 1.00 | 18.3 | 1489 | 1344 | 0.5 |
| 31 Oct 2011 | 8.23 | 48.0 | 222.8 | 9.4 | 196.9 | 8.6 | 17.5 | 1555 | 1403 | 0.5 |
| 2 Nov 2011 | 5.19 | 29.8 | 72.77 | 2.75 | 74.86 | 2.8 | 19.9 | 1367 | 1234 | 0.5 |
| 2 Nov 2011 | 8.23 | 48.0 | 193.6 | 6.7 | 173.0 | 5.8 | 18.5 | 1473 | 1329 | 0.5 |
| 4 Nov 2011 | 0.84 | 7.0 | 11.80 | 0.56 | 10.84 | 0.42 | 19.5 | 1396 | 1260 | 0.55 |
| 4 Nov 2011 | 9.38 | 56.4 | 373.1 | 19.5 | 318.1 | 11.4 | 19.2 | 1419 | 1280 | 0.5 |
| 8 Nov 2011 | 5.19 | 29.8 | 63.86 | 2.58 | 58.13 | 1.75 | 17.0 | 1598 | 1442 | 0.5 |
| 10 Nov 2011 | 11.5 | 67.1 | 726.2 | 92.6 | 505.3 | 60.7 | 17.25 | 1577 | 1422 | 0.5 |
| 11 Nov 2011 | 9.38 | 56.4 | n.m. | n.m. | 299.9 | 9.7 | 17.25 | 1577 | 1422 | 0.5 |
| 14 Nov 2011 | 0.84 | 7.0 | 6.77 | 2.18 | 7.90 | 0.65 | 17.0 | 1598 | 1442 | 0.55 |
| 15 Nov 2011 | 7.25 | 40.7 | 132.4 | 5.9 | 134.7 | 4.8 | 16.2 | 1671 | 1507 | 0.5 |
| 16 Nov 2011 | 2.34 | 16.7 | 30.5 | 1.1 | 26.98 | 1.0 | 14.5 | 1837 | 1657 | 0.5 |
| 16 Nov 2011 | 7.25 | 40.7 | 114.9 | 6.2 | 133.1 | 5.3 | 13.25 | 1973 | 1779 | 0.5 |
| 17 Nov 2011 | 1.50 | 12.1 | 13.1 | 1.4 | 15.29 | 0.48 | 14.1 | 1880 | 1695 | 0.55 |
| 17 Nov 2011 | 3.10 | 23.7 | 42.3 | 5.3 | 45.37 | 3.71 | 13.3 | 1967 | 1774 | 0.5 |
| 18 Nov 2011 | 0.84 | 7.0 | 7.75 | 0.65 | 7.42 | 0.34 | 14.15 | 1874 | 1690 | 0.55 |
| 19 Nov 2011 | 5.19 | 29.8 | 55.6 | 2.8 | 55.59 | 2.8 | 15.2 | 1766 | 1593 | 0.5 |
| 19 Nov 2011 | 11.5 | 67.1 | 671.7 | 45.0 | 543.6 | 34.2 | 17.25 | 1577 | 1422 | 0.5 |





OSD
10, 1971–1996, 2013

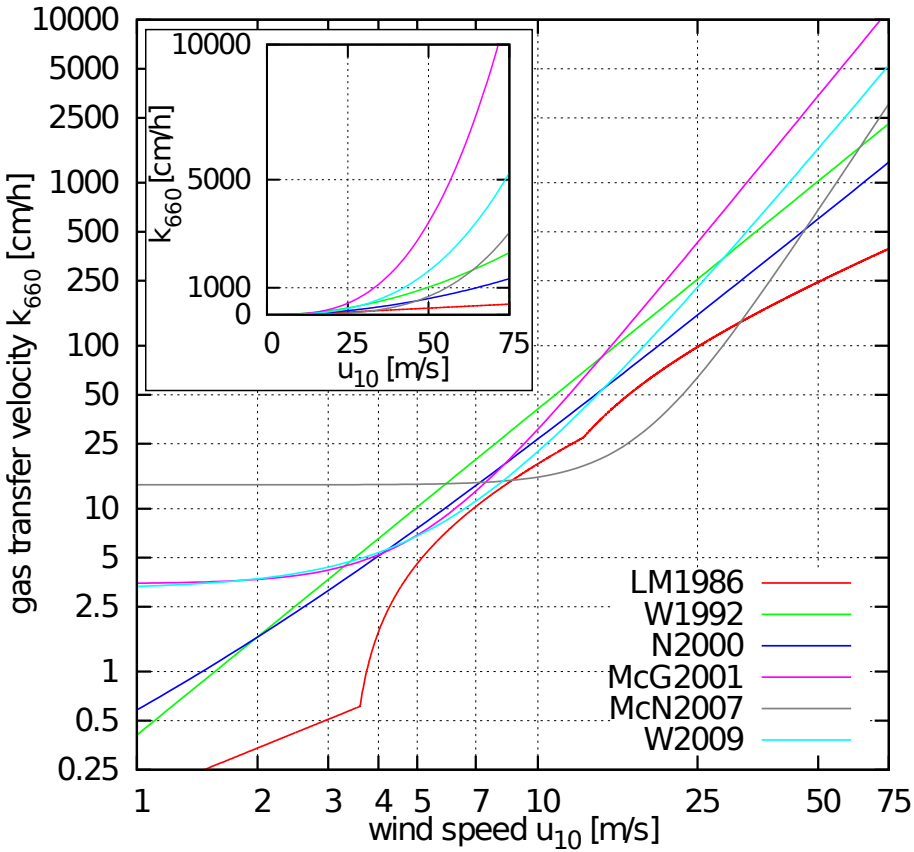


**Fig. 1.** Some commonly used gas transfer – wind speed parameterizations in a double logarithmic plot. The insert shows the same, but with linear axes. LM1986: Liss and Merlivat (1986), W1992: Wanninkhof (1992), N2000: Nightingale et al. (2000), McG2001: McGillis et al. (2001) and W2009: Wanninkhof et al. (2009). The parameterization by McNeil and D'Asaro (2007) (McN2007) is the only one developed for hurricane wind speeds.





OSD
10, 1971–1996, 2013

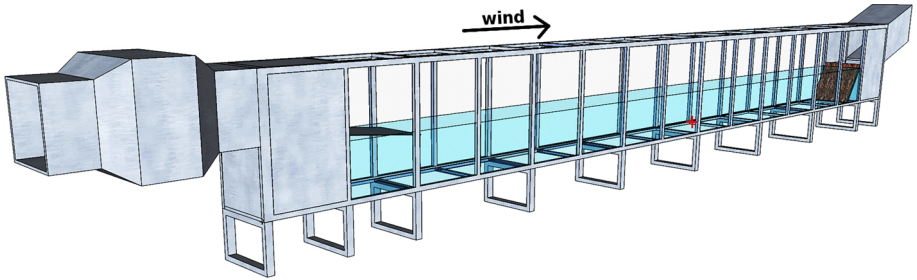


**Fig. 2.** Schematic view of the flume section of the Kyoto High-Speed Wind-Wave Tank. Not shown is the radial fan producing the wind (left side). The red cross marks the approximate sampling position.





OSD
10, 1971–1996, 2013

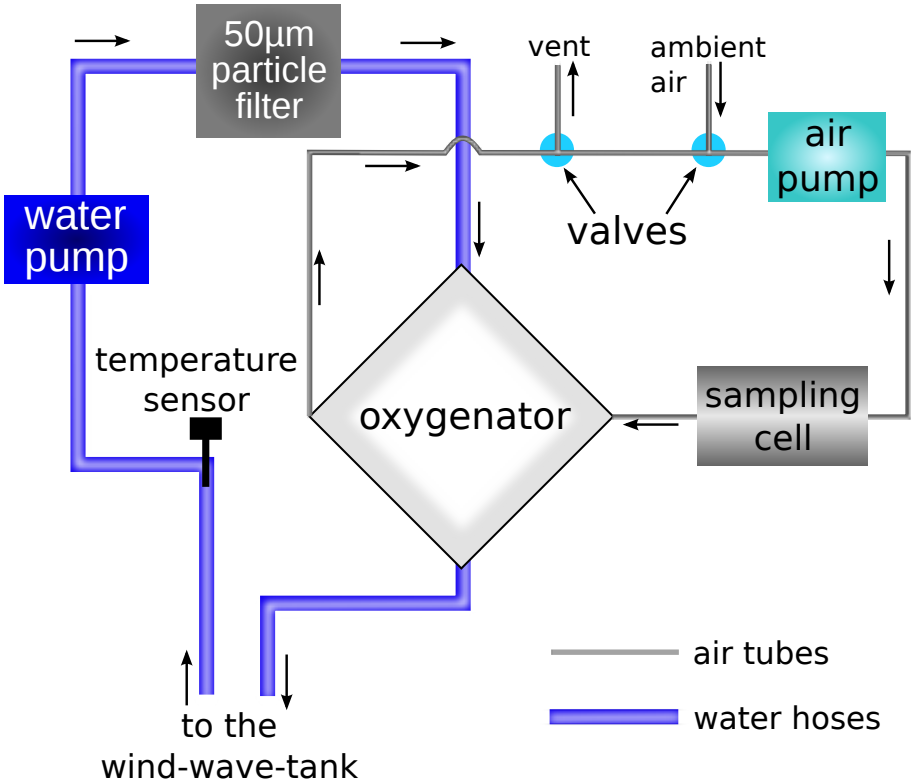


**Fig. 3.** Gas extraction setup. Water pumped from the wind-wave tank is equilibrated with air using an oxygenator. The air is continuously cycled between the oxygenator and the UV-spectroscopic measuring cell. The valves allow background sampling and are closed during measurements.





OSD
10, 1971–1996, 2013

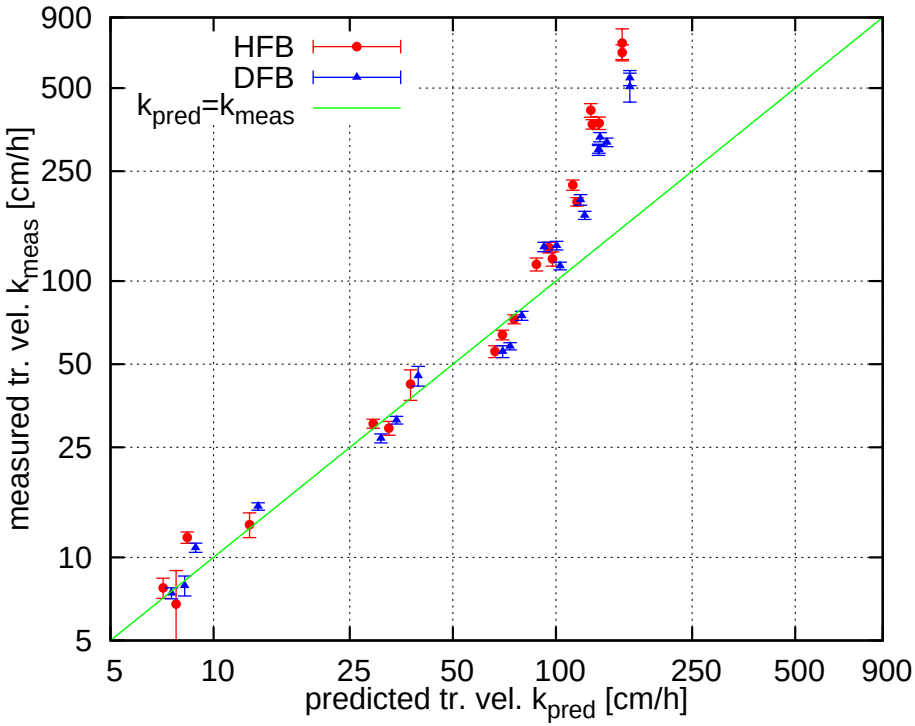


**Fig. 4.** Measured transfer velocities $k_{meas}$ for HFB and DFB as well as the transfer velocities $k_{pred}$ predicted by Eq. (2) in a double logarithmic plot.





OSD
10, 1971–1996, 2013

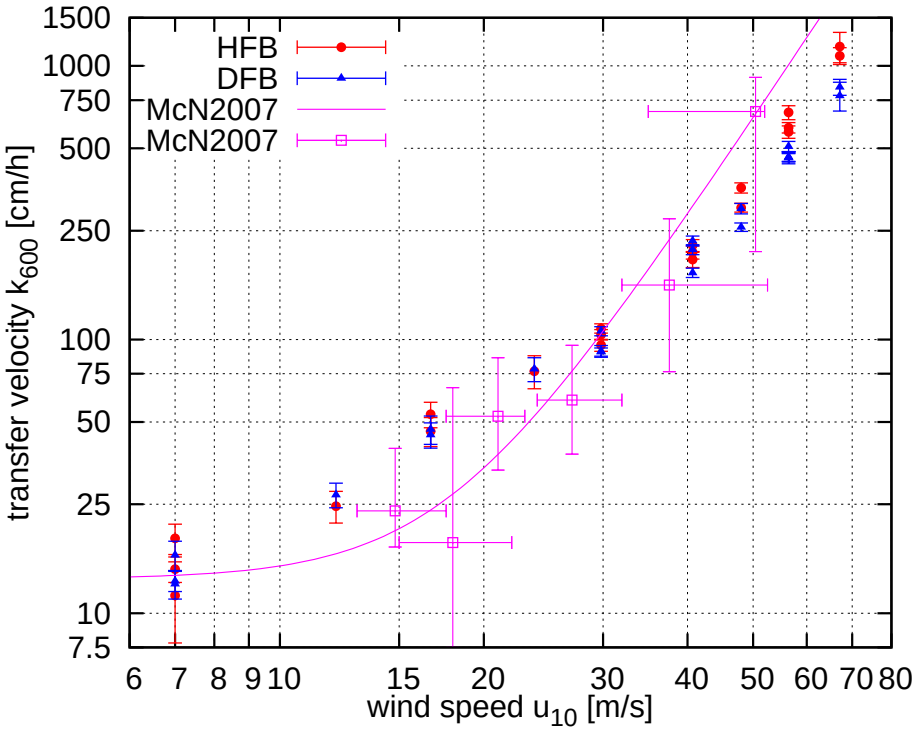


**Fig. 5.** Measured transfer velocities for HFB and DFB, compared to the data and parameterization by McNeil and D'Asaro (2007), all scaled to a Schmidt number of 600, in a double logarithmic plot.





OSD
10, 1971–1996, 2013

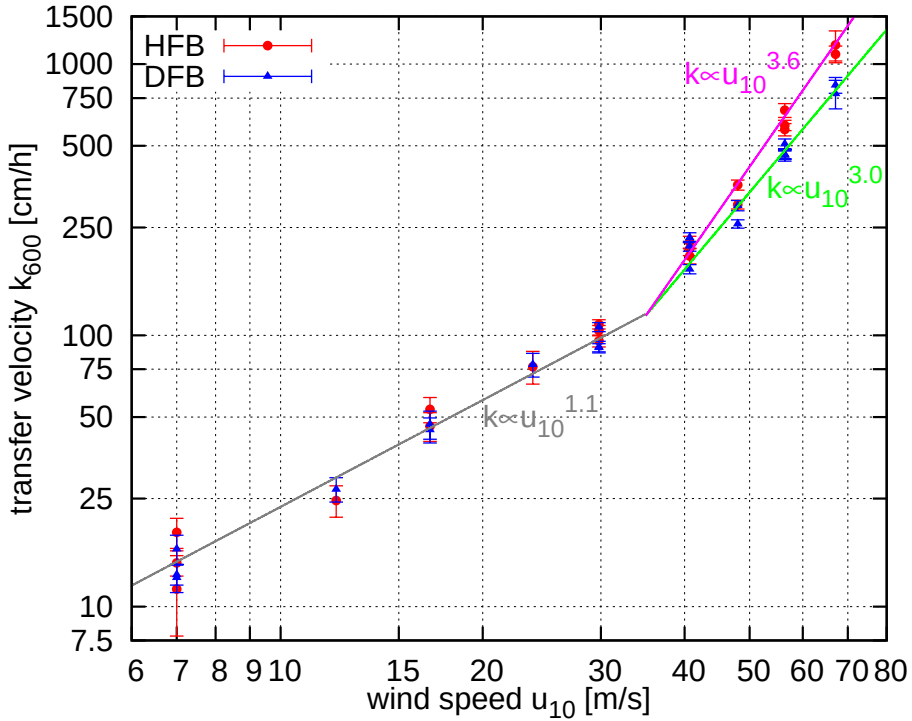


**Fig. 6.** Measured transfer velocities for HFB and DFB scaled to a Schmidt number of 600. Also shown are lines indicating proportionalities of the transfer velocities $k_{600}$ to $u_{10}^{x}$ with $x$ depending on the wind speed range and the tracer.





OSD
10, 1971–1996, 2013

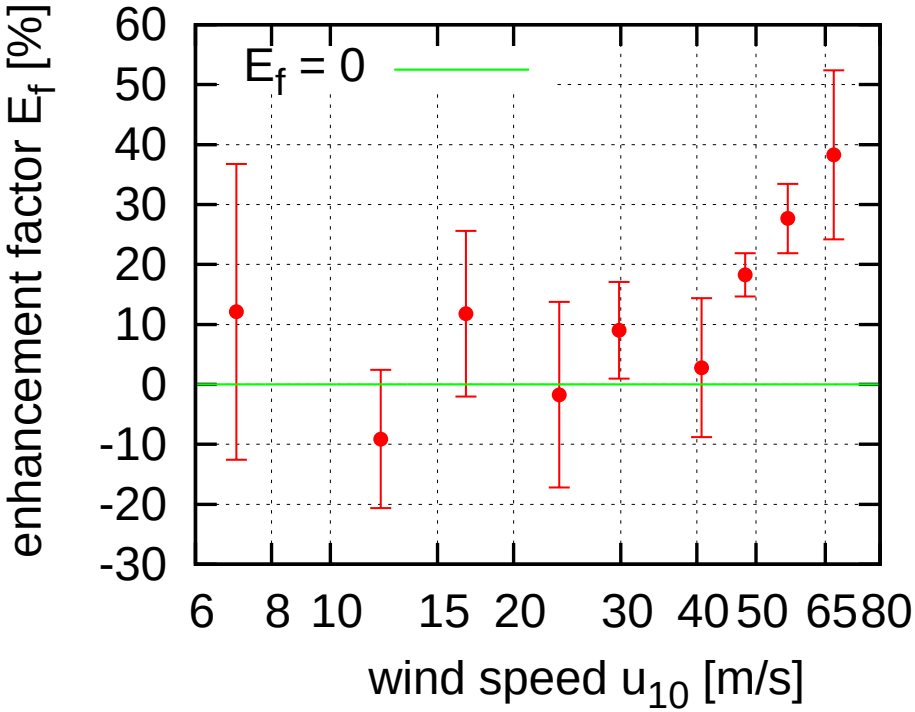


**Fig. 7.** Mean enhancement of the transfer velocity of HFB over that of DFB, both scaled to a Schmidt number of 600. An $E_f$ of 0 means no enhancement.





OSD
10, 1971–1996, 2013

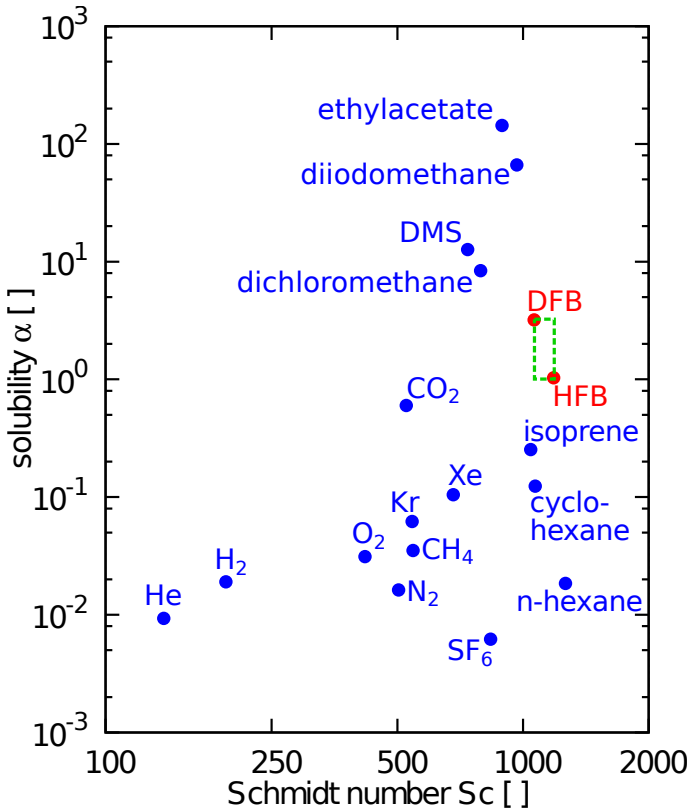


**Fig. 8.** Double logarithmic Schmidt number – solubility diagram of some environmentally important tracers for a temperature of 25 °C. The tracers used in this study, hexafluorobenzene (HFB) and 1,4-difluorobenzene (DFB), cover a very limited parameter range, marked by the dashed green rectangle.





OSD
10, 1971–1996, 2013